FERMILAB-CONF-08-592-E

MEASUREMENT OF TOTAL ACTIVE NEUTRINO FLUX IN THE MINOS DETECTORS

BRIAN J. REBEL
Fermilab, PO Box 500
Batavia, IL 60510, USA
E-mail: brebel@fnal.gov

for

THE MINOS COLLABORATION

ABSTRACT

The neutral-current neutrino interactions from a neutrino beam produced by the Fermilab Main Injector have been measured using two detectors separated by 734 km. As oscillations among active flavors leave the total number of $\nu_e + \nu_\mu + \nu_\tau$ unchanged, this measurement characterizes the extent that the previously observed ν_μ disappearance is due only to mixing with ν_e and ν_τ rather than mixing that includes a non-interacting sterile particle. The neutral-current event rate is consistent with expectations limiting any depletion of the total low-energy active neutrino flux to below 35% at 90% confidence level. The neutral-current event rate is also analyzed in the context of a model with one sterile neutrino limiting the coupling of the sterile neutrino with the third mass eigenstate to be less than 0.45 at 90% confidence level.

1. Introduction

Several experiments in the last decade have provided evidence for ν_μ and ν_e disappearance as the neutrinos propagate from the point of production [1)]. The Super-Kamiokande experiment has reported that $\nu_\mu \rightarrow \nu_\tau$ oscillation is the most likely explanation for ν_μ disappearance [2)]. Measurements of solar ν_e showed that the disappearance of those neutrinos is due to matter enhanced oscillations [3)]. The KamLAND reactor experiment demonstrated vacuum mixing of $\overline{\nu}_e$ [4)].

These results can be interpreted as mixing among the active flavors, those that couple to the electroweak current. Precise measurements of the decay width of the Z^0 boson showed that there are only three light active neutrinos [5)], but they do not exclude the existence of neutrinos that do not couple to the electroweak current. The existence of "sterile" neutrinos could clarify several outstanding problems in particle physics and astrophysics. For example, sterile neutrinos with masses at the eV energy scale can participate in the seesaw mechanism that introduces neutrino masses [6,7)] as well as aiding in heavy element nucleosynthesis in supernovae [6)]. The SNO experiment has shown that the total flux of active neutrinos from the Sun agrees with the expectation from solar models [8)] limiting the extent to which the first or second neutrino mass eigenstates mix with a sterile neutrino.

The MINOS experiment has reported a significant deficit of ν_μ at its far detector for $E_\nu < 6$ GeV relative to the near detector through measurement of the rate of ν_μ

charged-current (CC) interactions [9,10]. If this deficit is due solely to conversions of ν_μ to $\nu_e + \nu_\tau$, then the rate of neutral-current (NC) interactions at the far detector would remain unchanged. If any of the ν_μ convert to a sterile state, then the NC rate would be suppressed. This analysis reports a measurement of NC interactions in the MINOS near and far detectors limiting the rate of conversion of active to sterile states using a model independent method. The data are then compared to a specific model for mixing between the three active neutrinos and one light sterile neutrino limiting the amount a sterile neutrino couples to the third mass eigenstate.

2. Neutrino Beam and Detectors

The NuMI neutrino beam is produced using 120 GeV/c protons from the Fermilab Main Injector. The energy spectrum of the neutrino beam can be changed by adjusting the current of the horns and the position of the target relative to the focussing horns. The data used in this analysis come from the low energy beam configuration with an exposure of 2.46×10^{20} protons on target in the far detector and matches the data analyzed in [10].

The MINOS detectors are steel-scintillator tracking-calorimeters [11]. The vertically oriented detector planes are laminations of 2.54 cm thick steel and 1 cm thick plastic scintillator. The scintillator layer is comprised of 4.1 cm wide strips that are coupled via wavelength-shifting fiber to one pixel of a multi-annode photomultiplier-tube [12,13]. The detectors are magnetized to an average field of 1.3(1.2) T in the far(near) detector. The MINOS near detector is located 1.04 km downstream of the target, has a mass of 0.98 kt, and lies 103 m underground at Fermilab. The far detector is 734 km downstream of the near detector, has a mass of 5.4 kt, and is located in the Soudan Underground Laboratory, 705 m below the surface. The fiducial mass of the near detector used for this analysis is 27 t and the fiducial mass of the far detector is 3.8 kt.

Hadronic showers resulting from NC interactions generate signal on 12 strips for every GeV deposited. All events must have at least 4 strips with a signal in order to be considered in the analysis. Individual scintillator strips are grouped into either reconstructed tracks or showers, which are combined into events. Charged-current interactions are identified by the presence of a track that may or may not be associated with a shower. Neutral-current interactions are typically made up of a single hadronic shower, although the reconstruction may identify a track in the event. Such tracks could come from pions, but are more likely reconstruction artifacts. The vertex for each event used in the analysis was required to be sufficiently far from an edge of the detector to assure that the final-state hadronic showers were well contained within the fully sampled portion of the detectors.

The near detector data are used to predict the number of expected events in the far detector, but the prediction is complicated by the high rate environment at

the near detector. Timing and spatial information are used to separate individual neutrino interactions in the same spill, but the reconstruction program generally overestimates by 36% the number of interactions having $E_{reco} < 1$ GeV. A series of selection requirements making use of event topology and timing are used to decrease this background. Events must be separated by at least 40 ns and events that occur within 120 ns of each other must be separated by at least 1 m in the longitudinal direction [14]. After applying these criteria, the remaining background from poorly reconstructed events with $E_{reco} < 1$ GeV is 7% and it is treated as a systematic uncertainty below.

The neutrino interactions from the NuMI beam in the far detector are identified using a window around the GPS time stamp of the spills of $-2 < t < 12$ μs where t is the time of the spill. Given the low rate of neutrino interactions in the far detector, spurious events from noise, cosmic ray muons and poor event reconstruction that are coincident with the beam spills can introduce backgrounds to the analysis. Additional event selections are used to remove such events from the data set. The background due to cosmic ray muons that are coincident with the spill times has been shown to be negligible [10].

3. NC-like Event Selection and Far Detector Prediction

An event surviving the selection process in either detector was classified as NC-like if it has a reconstructed shower, is shorter than 60 planes and has no track extending more than 5 planes beyond the shower. Distributions of these event-topology parameters for near detector events are shown in Fig. 1. The major background in the spectrum of NC-like events comes from highly inelastic ν_μ-CC interactions. The reconstructed energy, E_{reco}, spectrum of NC-like events in the near detector is shown in Fig. 2 along with the Monte Carlo prediction.

The near detector data are used to directly correct the Monte Carlo estimate of the NC-like event spectrum at the far detector. To make this correction, the Monte Carlo simulation is used to predict the ratio of event yields in the far detector and near detector as a function of energy. This ratio is multiplied by the observed energy spectrum in the near detector to produce a corrected far detector prediction. The true energy of the simulated neutrinos in each reconstructed energy bin of the prediction is used to determine the effect of oscillations for that range of reconstructed energy. The methods for identifying NC-like events and predicting the far detector spectra were developed and tested using near detector data only. To avoid biases the analysis was finalized prior to examining data in the far detector.

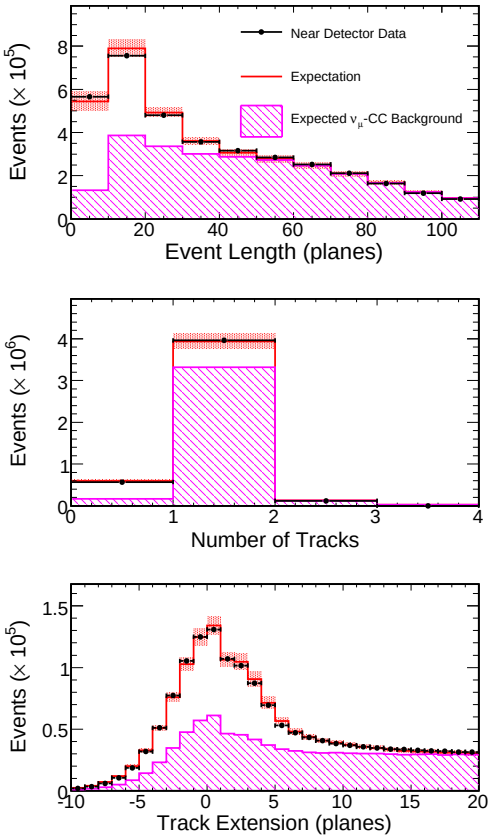

Figure 1: Distributions of event-topology parameters used to separate NC-like from CC-like events. Data from the near detector (solid points) are shown superposed on the total Monte Carlo expectation. The hatched distributions show the ν_μ-CC background as determined by the Monte Carlo simulation. The systematic uncertainty for the Monte Carlo expectation is shown by the shaded band.

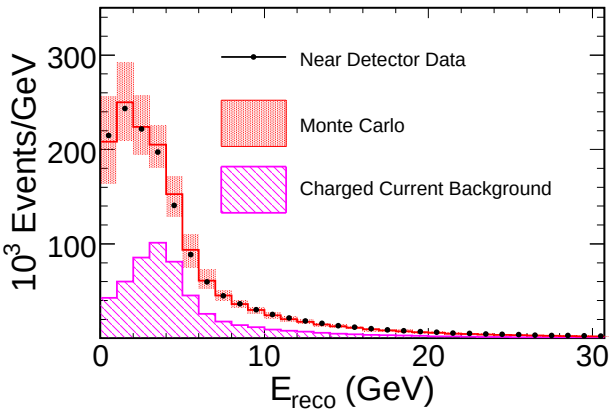

Figure 2: The reconstructed energy spectrum for NC-like events in the near detector. The data (solid points) and the Monte Carlo expectation (solid histogram) are shown. The hatched distribution shows the expected ν_μ-CC background. The systematic uncertainty for the Monte Carlo expectation is shown by the shaded band.

4. Three Neutrino Analysis

Figure 3 shows the measured and extrapolated E_{reco}, spectra at the far detector. These spectra are compared using a statistic, f, which measures the fraction of active neutrinos that disappear between the near detector and far detector:

$$f \equiv 1 - \frac{N_{Data} - B_{CC}}{S_{NC}}, \tag{1}$$

where, within a given energy range, N_{Data} is the measured event count, B_{CC} is the extrapolated CC background, and S_{NC} is the extrapolated number of NC interactions. The values of S_{NC} and B_{CC} are calculated assuming oscillation among the three active neutrinos. The parameter f is a model independent method to determine the coupling between active and sterile neutrinos as it makes no assumptions on the number of sterile neutrinos or their corresponding mass eigenstates. The previous measurement by MINOS showed that ν_μ with energies below 6 GeV disappeared between the near and far detectors [15]. As the neutrino energy is not measured for NC interactions, this analysis separates the events into two samples based on the reconstructed energy, $0-3$ GeV and $3-120$ GeV. The Monte Carlo simulation shows that 85% of the events in the lower energy sample are from neutrinos with $E < 6$ GeV. Integrating from $0-3$ GeV yields $N_{Data} = 100$, $B_{CC} = 14.0$, and $S_{NC} = 101.1$ giving

$$f_{low} = 0.15 \pm 0.10(\text{stat})^{+0.06}_{-0.07}(\text{syst}). \tag{2}$$

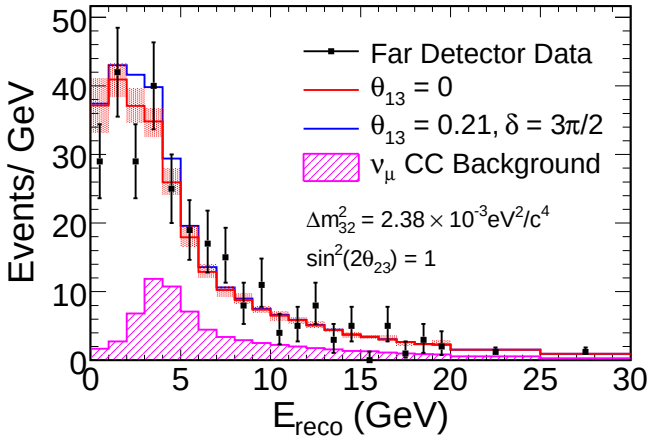

Figure 3: Spectra of observed NC-like events in the far detector along with predictions for the two oscillation hypotheses described in the text. The systematic uncertainty in the predicted rates is indicated by the extent of the filled regions in each bin.

For the range $3 - 120$ GeV, $N_{Data} = 191$, $B_{CC} = 79.4$, and $S_{NC} = 98.1$ giving

$$f_{high} = -0.14 \pm 0.14(\text{stat})^{+0.13}_{-0.14}(\text{syst}). \quad (3)$$

According to the simulation, the median energy of neutrinos producing interactions with $E_{reco} < 3$ GeV is 3 GeV and the median energy of neutrinos producing interactions with $3 < E_{reco} < 120$ GeV is 8 GeV.

The sources of systematic uncertainty in f_{low} and f_{high} are listed in Table 1. The absolute scale of the hadronic energy is known to within 11%; 10% resulting from uncertainties in the final-state interactions in the nucleus and 6% uncertainty from detector response. The total uncertainty in f_{low} from the absolute energy scale is 0.002. The relative calibration of the hadronic energy between the detectors has an uncertainty of 3% [10] resulting in an uncertainty in f_{low} of 0.03. The relative normalization between the near detector and far detector has an uncertainty of 4%, causing an uncertainty of 0.04 in f_{low}. The event count in the near detector has an uncertainty of 15% for $E_{reco} < 0.5$ GeV; 3% for events with $0.5 < E_{reco} < 1$ GeV; and is negligible for $E_{reco} > 1$ GeV. The resulting uncertainty in f_{low} is 0.02.

The background is dominated by ν_μ-CC interactions misidentified as NC-like. The uncertainty on the size of the ν_μ-CC background was determined from near detector data using the flexibility of the NuMI beamline [10] to vary the peak of the misidentified ν_μ-CC background in the reconstructed energy spectrum. Comparisons of the different spectra showed the background to be 15% for all reconstructed energies. The far detector predictions include $\nu_\mu \rightarrow \nu_\tau$ oscillations using the MINOS measured values of $\Delta m^2_{32} = 2.38 \times 10^{-3}$ eV^2 and $\theta_{23} = \pi/4$ [15,?]. Variations in the oscillation parameters changes the ν_μ-CC background in the far detector up to 10% for

Table 1: Sources of systematic uncertainties considered in this analysis. The table shows the uncertainty in f due to each source. The uncertainty due to the near detector selection is only for events with $E_{reco} < 1$ GeV. Also shown are the values of f_{low} and f_{high} for the case without ν_e appearance.

	0 – 3 GeV	3 – 120 GeV
Absolute E_{had}	± 0.00	± 0.06
Relative E_{had}	± 0.03	± 0.03
Normalization	± 0.04	$^{+0.10}_{-0.11}$
Near detector selection	± 0.02	0
ν_μ CC background	$^{+0.04}_{-0.05}$	± 0.04
Total:	$^{+0.06}_{-0.07}$	$^{+0.13}_{-0.14}$
$f_{low} = 0.15 \pm 0.10(\text{stat.})^{+0.06}_{-0.07}(\text{syst.})$		[0 – 3 GeV]
$f_{high} = -0.14 \pm 0.14(\text{stat.})^{+0.12}_{-0.13}(\text{syst.})$		[3 – 120 GeV]

the 1σ range previously reported by MINOS [15]. Uncertainties in these backgrounds contribute 0.05 to the uncertainty in f_{low}.

Because the NC-like selection criteria identify ν_e-CC interactions as NC-like with nearly 100% efficiency, the potential background from $\nu_\mu \rightarrow \nu_e$ oscillations is also considered. An upper limit for the ν_e-CC rate was estimated using the normal mass hierarchy with $\theta_{12} = 0.61$ rad, $\theta_{13} = 0.21$ rad, $\delta = 3\pi/2$ rad, $\Delta m^2_{21} = 7.59 \times 10^{-5}\text{eV}^2$, and $\Delta m^2_{32} = 2.38 \times 10^3$ eV^2 [16,15]. The choice of θ_{13} corresponds to the 90% confidence level upper limit for $\Delta m^2_{32} = 2.38 \times 10^3$ eV^2 [17]. Under these assumptions $f_{low} = 0.20 \pm 0.09(\text{stat})^{+0.06}_{-0.07}(\text{syst})$ and $f_{high} = -0.01 \pm 0.14(\text{stat})^{+0.13}_{-0.14}(\text{syst})$.

The measured value of f_{low} is consistent with 0 to within 1.23σ. The probability of finding $f_{low} \geq 0.15$ was determined to be 7% using simulated experiments. This result indicates the presence of ν_e and ν_τ in the beam at the far detector. Lacking evidence for conversion between active and sterile states, an upper bound limiting the average probability for active to sterile conversion is set to be below 35% at 90% confidence level at low energies.

5. Four Neutrino Analysis

The measured value of f_{low} limits the amount of mixing between active and sterile neutrinos in a model independent way. It is also useful to compare the data to a specific model for mixing between active and sterile neutrinos. A model describing mixing between active and sterile neutrinos that introduces a single sterile neutrino and a corresponding fourth mass eigenstate was chosen and the mixing matrix for this model is

$$U = \begin{bmatrix} U_{e1} & U_{e2} & U_{e3} & U_{e4} \\ U_{\mu 1} & U_{\mu 2} & U_{\mu 3} & U_{\mu 4} \\ U_{\tau 1} & U_{\tau 2} & U_{\tau 3} & U_{\tau 4} \\ U_{s1} & U_{s2} & U_{s3} & U_{s4} \end{bmatrix}, \quad (4)$$

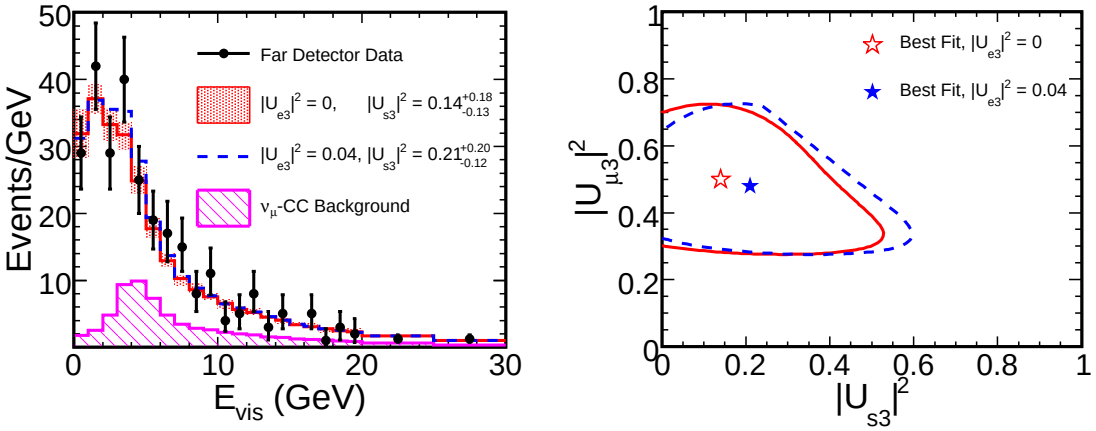

Figure 4: Spectra of observed NC-like events in the far detector along with the best fit spectra for the model with mixing between active and sterile neutrinos (left) and 90% confidence level contours for the best fit values (right).

where $U_{\alpha i}$ is the element describing the coupling between flavor α and mass state i. Because the solar neutrino results strongly limit mixing between the first or second mass eigenstates and sterile neutrinos, it is assumed that $|U_{s1}|^2 = |U_{s2}|^2 = 0$. The mass splitting between the first and second mass eigenstates is too small to contribute to oscillations at the energies and baseline of the MINOS experiment and can be neglected in this analysis. The final assumption of the model is that the first and fourth mass eigenstates have nearly degenerate masses. Given these assumptions, the probability for ν_μ conversion to any flavor state is

$$\begin{aligned} P_{\nu_\mu \to \nu_\mu} &= 1 - 4|U_{\mu 3}|^2(1 - |U_{\mu 3}|^2)\sin^2(1.27\Delta m^2_{31} L/E) \\ P_{\nu_\mu \to \nu_e} &= 4|U_{\mu 3}|^2|U_{e3}|^2\sin^2(1.27\Delta m^2_{31} L/E) \\ P_{\nu_\mu \to \nu_s} &= 4|U_{\mu 3}|^2|U_{s3}|^2\sin^2(1.27\Delta m^2_{31} L/E) \\ P_{\nu_\mu \to \nu_\tau} &= 1 - P_{\nu_\mu \to \nu_\mu} - P_{\nu_\mu \to \nu_e} - P_{\nu_\mu \to \nu_s}, \end{aligned} \tag{5}$$

where Δm^2_{31} is the difference in the square of the masses of the first and third mass eigenstates, L is the baseline of the experiment, and E is the energy of the neutrino.

The data were compared to expectations based on eq. (5). The comparison varied values of Δm^2_{31}, $|U_{\mu 3}|^2$, and $|U_{s3}|^2$ to obtain the best agreement between the data and expectation. The sources of systematic uncertainty listed in Table 1 were included in the comparison as nuisance parameters. The data were compared to expectations with and without ν_e appearance, that is $|U_{e3}|^2 = 0$ and at the CHOOZ limit, $|U_{e3}|^2 = 0.04$. The left panel of Fig. 4 shows the data and best fit spectra for this model. The best fit values for $|U_{e3}|^2 = 0$ are $|U_{s3}|^2 = 0.14^{+0.18}_{-0.13}$ and $|U_{\mu 3}|^2 = 0.50^{+0.16}_{-0.15}$; with ν_e appearance the values are $|U_{s3}|^2 = 0.21^{+0.20}_{-0.12}$ and $|U_{\mu 3}|^2 = 0.48^{+0.18}_{-0.12}$. The best fit values of Δm^2_{31}

are consistent with the previously reported values using ν_μ-CC interactions. The right panel of the figure shows the 90% confidence level contours in the $|U_{s3}|^2 - |U_{\mu 3}|^2$ plane. The value of $|U_{s3}|^2$ is limited to be less than 0.45 at the 90% confidence level when there is no appearance of ν_e in the beam. The results are consistent with the values of f_{low} reported above.

6. Conclusions

In conclusion, the rates of NC-like events in the near and far detectors are consistent with oscillations occurring only between the active flavors and are evidence for ν_τ and ν_e appearing in the NuMI beam. The amount of conversion between active and sterile neutrinos has been limited to less than 35% at the 90% confidence level using a model independent approach. When the data are compared to the expectations for a model including a fourth sterile neutrino, the coupling between the sterile neutrino and the third mass eigenstate, $|U_{s3}|^2$, is limited to be less than 0.45 at the 90% confidence level.

7. Acknowledgements

This work was supported by the U.S. Department of Energy, the U.K. Science and Technology Facilities Council, the U.S. National Science Foundation, and the State and University of Minnesota. We are grateful to the Minnesota Department of Natural Resources, the crew of the Soudan Underground Laboratory, and the staff of Fermilab for their contribution to this effort.

8. References

1) R. Davis et al., Phys. Rev. Lett. **9**, 36 (1962); P. Anselmann et al., Phys. Lett. **B285**, 376 (1992); R. Becker-Szendy et al., Phys. Rev. **D46**, 3720 (1992);K. S. Hirata et al., Phys. Lett. **B280**, 146 (1992); J. N. Abdurashitov et al., Phys. Lett. **B328**, 234 (1994); M. Sanchez et al., Phys. Rev. **D68**, 113004 (2003); M. H. Ahn et al, Phys. Rev. **D74**, 072003 (2006
2) J. Hosaka et al., Phys. Rev. **D74**, 032002 (2006); K. Abe et al., Phys. Rev. Lett. **97**, 171801 (2006)
3) Y. Fukuda et al., Phys. Rev. Lett. **86**, 5651 (2001); Q. R. Ahmad et al., Phys. Rev. Lett. **89**, 011301 (2006); P. Anselmann et al., Phys. Lett. **B285**, 376 (1992); J. N. Abdurashitov et al., Phys. Rev. Lett. **B328**, 234 (1994)
4) A. Kozlov, Nucl. Phys. Proc. Suppl. **149** (2005)
5) M. Acciarri et al., Phys. Lett. **B431**, 199 (1998); P. Abreu et al., Z. Phys. **C74**, 577 (1997); R. Akers et al. Z. Phys **C65**, 47 (1995); D. Buskulic et al., Phys. Lett. **B313**, 520 (1993); G. S. Abrams et al., Phys. Rev. Lett **63**, 2173

(1989)
6) A. de Gouvea et al., Phys. Rev. **D75**, 013003 (2007)
7) A. Kusenko, AIP Conf. Proc. **917**, 58 (2007)
8) Q. R. Ahmad et al., Phys. Rev. Lett. **89**, 011301 (2002)
9) D. G. Michael et al., Phys. Rev. Lett. **97**, 191801 (2006)
10) P. Adamson et al., Phys. Rev. **D77**, 072002 (2008)
11) D. G. Michael et al., Nucl. Instr. Meth. *to be submitted* (2008)
12) N. Tagg et al., Nucl. Instr. Meth. **A539**, 668 (2005)
13) K. Lang et al., Nucl. Instr. Meth. **A545**, 852 (2005)
14) T. Raufer, Ph.D. Thesis, Oxford University (2007)
15) MINOS, arXiv:0708.1495 [hep-ex] (2007)
16) S. Abe et al., arXiv:0801.4589 [hep-ex] (2008)
17) M. Apollonio et al., Eur. Phys. J. **C27**, 331 (2003)